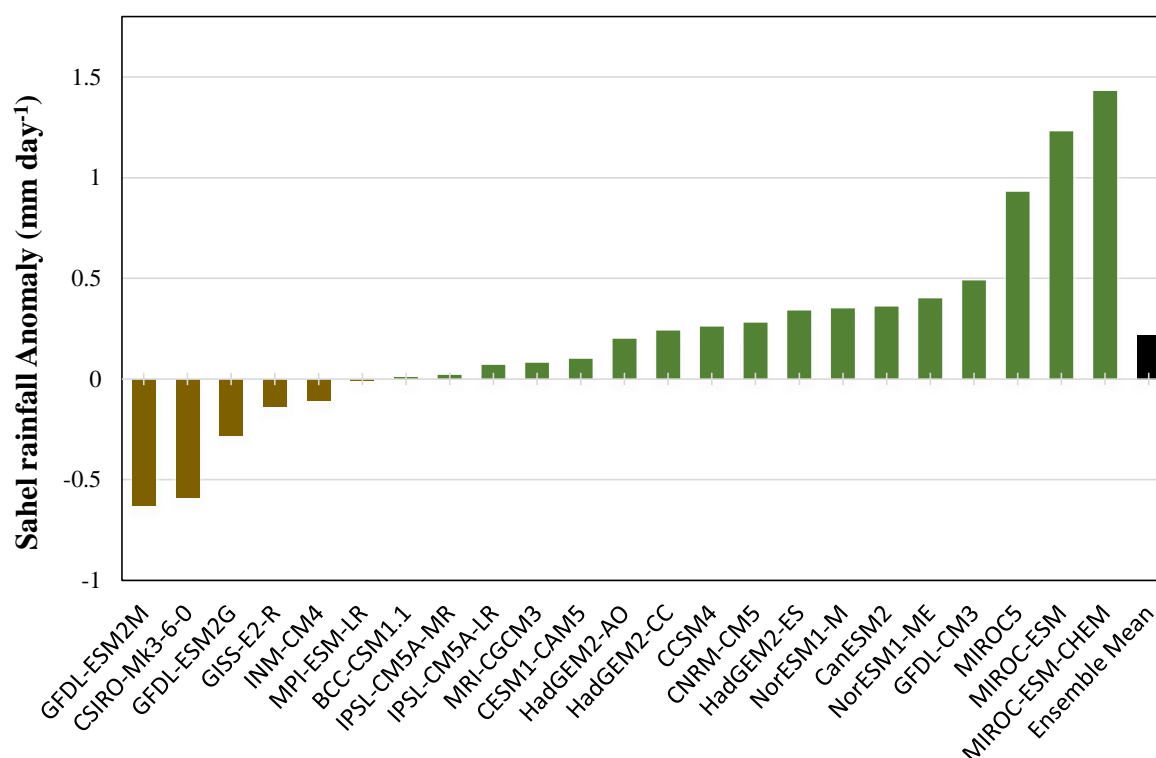
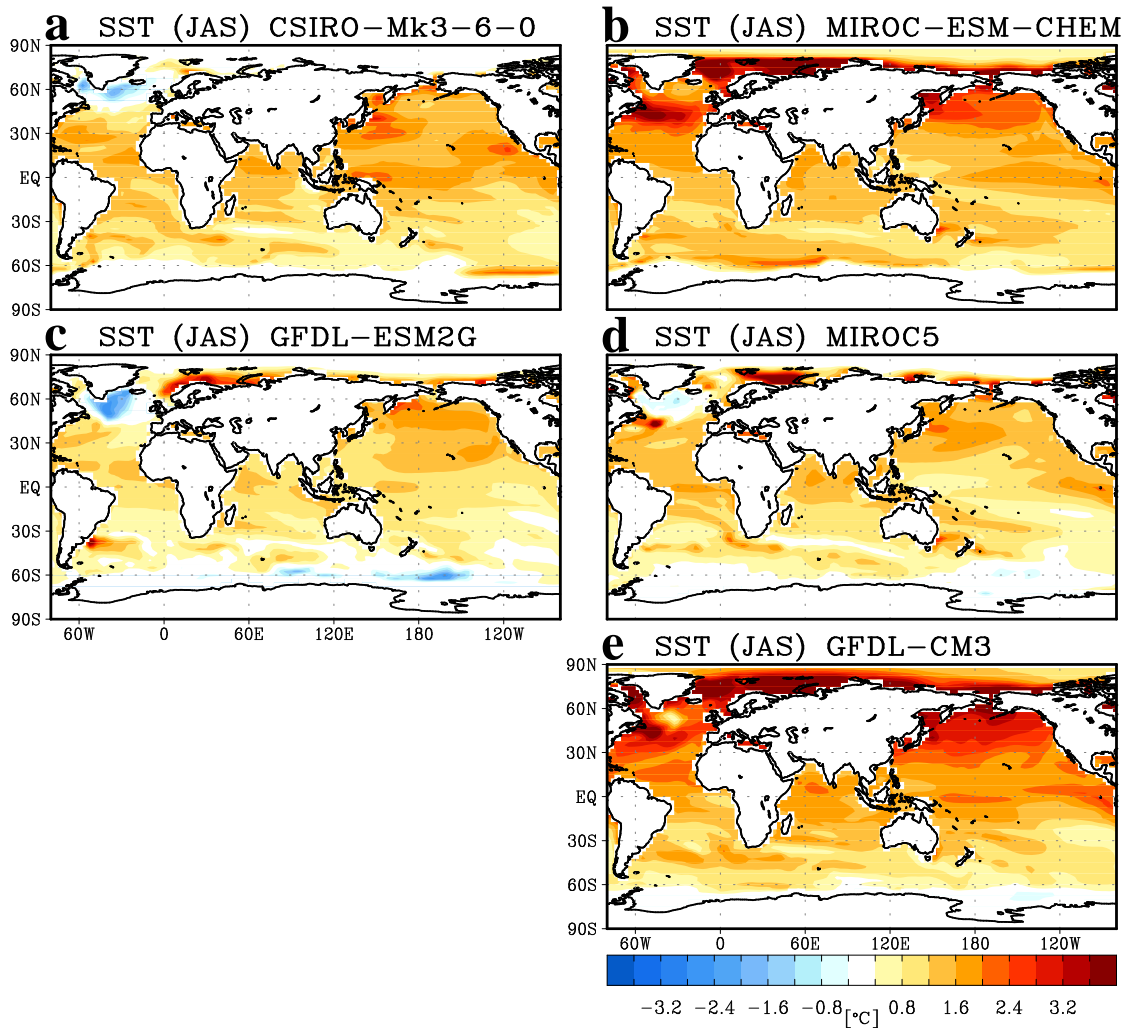


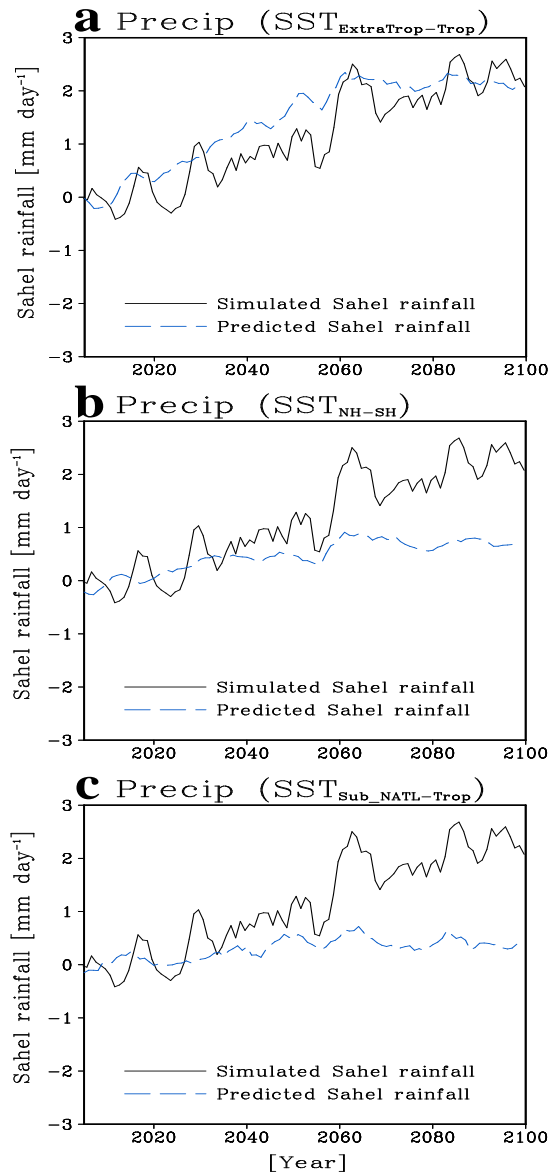
## Supplementary Figures



**Supplementary Figure 1| Uncertainty in future Sahel rainfall projections.** The future (2070-2099) JAS-mean Sahel rainfall anomalies from individual CMIP5 models. The anomalies are the differences from the mean of the historical run (1901-2005). Similar to previous results of CMIP3 (e.g. see Fig. 1 of Biasutti et al. 2008), GFDL-ESM and MIROC-ESM still project contradictory future rainfall anomalies, exhibiting a substantial drying ( $-0.63 \text{ mm day}^{-1}$ ) and a wetting ( $1.23 \text{ mm day}^{-1}$ ), respectively.

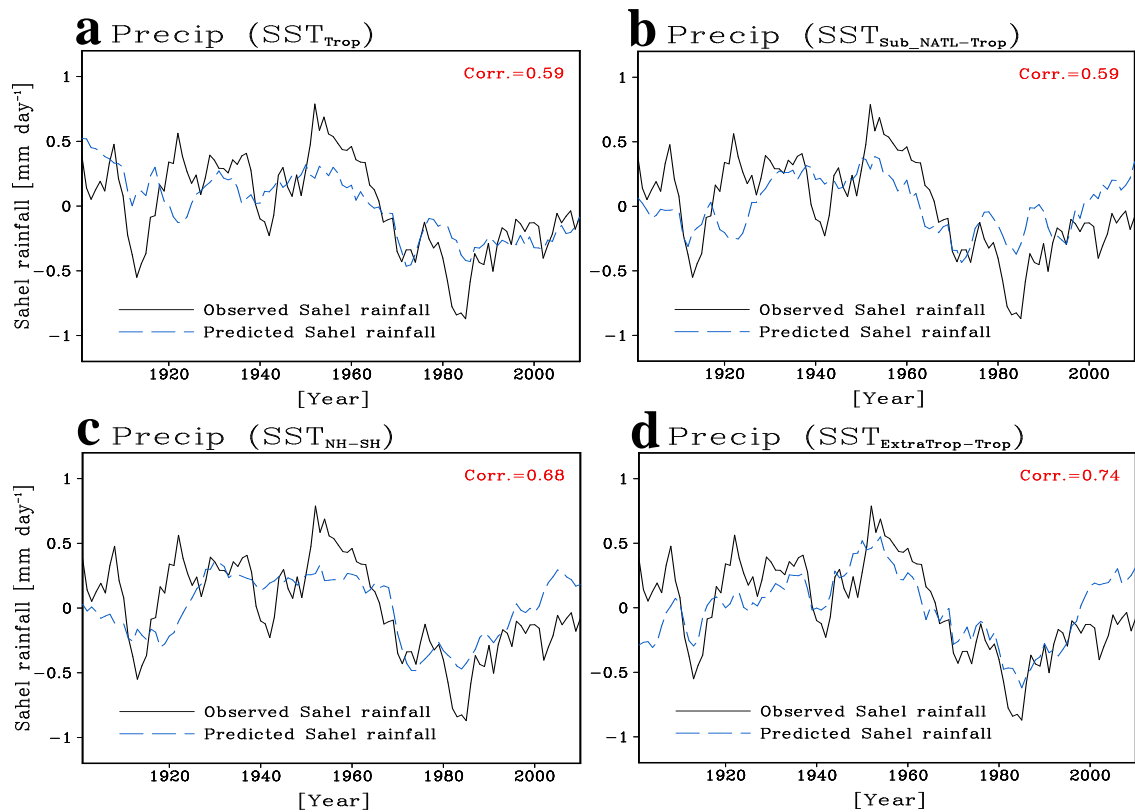


**Supplementary Figure 2| Future SST warming patterns in dry and wet models.** SST differences between the 21<sup>st</sup> century and 20<sup>th</sup> century for the models producing dry conditions (left panel) and for the models producing wet conditions (right panel) in future Sahel rainfall. Similar to a distinct difference in the amplitude of Northern Hemisphere (NH) extratropical warming between GFDL-ESM and MIROC-ESM, other CMIP5 models projecting significant future drying and wetting confirm such distinct extratropical SST warming relative to the tropical warming.

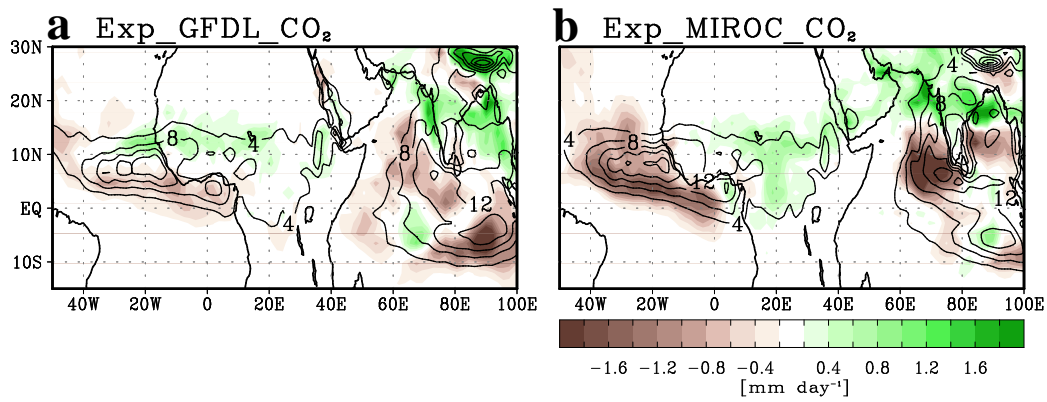


**Supplementary Figure 3 | Performance of different SST indices in predicting future Sahel rainfall.** **a-c**, Simulated Sahel rainfall (black line) from MIROC-ESM and linearly predicted Sahel rainfall (blue line) based on the difference between NH extratropical SST and tropical SST [(0°-360°E, 30°-75°N) minus (0°-360°E, 20°S-20°N)] (**a**), global interhemispheric SST gradient [(0°-360°E, 0°-90°N) minus (0°-360°E, 0°-90°S)] (**b**), and difference between subtropical North Atlantic SST and global tropical SST [(75°-15°W, 10°-40°N) minus (0°-360°E, 20°S-20°N)] (**c**). The regression coefficients of this linear model are calculated from the historical simulation (1901-2005). All time series data are smoothed using a five-year running mean. This performance comparison of different SST indices shows that our NH differential warming index can effectively capture the strong positive future

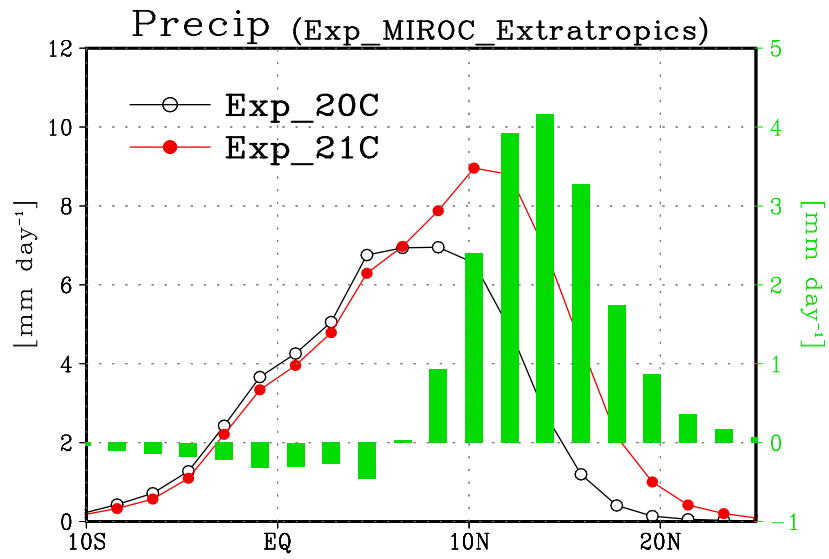
Sahel rainfall trend, whereas other supplementary indices show much weaker positive rainfall trends.



**Supplementary Figure 4| Performance of different SST indices in explaining historical Sahel rainfall.** a-c, Observed Sahel rainfall (black line) and linearly predicted Sahel rainfall (blue line) based on two tropical indices (tropical Atlantic and Indo-pacific) (a), difference between subtropical North Atlantic SST and global tropical SST [(75°-15°W, 10°-40°N) minus (0°-360°E, 20°S-20°N)] (b), global interhemispheric SST gradient [(0°-360°E, 0°-90°N) minus (0°-360°E, 0°-90°S)] (c), and difference between NH extratropical SST and tropical SST [(0°-360°E, 30°-75°N) minus (0°-360°E, 20°S-20°N)] (d). The correlation coefficients between observed and predicted rainfall are shown on the top right corner. All time series data are smoothed using a five-year running mean. The precipitation and sea surface temperature (SST) data are obtained from the Global Precipitation Climatology Center (GPCC) and the extended reconstructed SST version 3 (ERSST v3), respectively.



**Supplementary Figure 5| Direct radiative impacts of CO<sub>2</sub> increase on Sahel rainfall.** Mean differences in JAS-mean precipitation between two experiments prescribing 368 ppm and 538 ppm of CO<sub>2</sub> concentration. Both experiments are forced by twentieth century (1970-1999) climatological SST from GFDL-ESM2M (a) and MIROC-ESM (b) in CMIP5.



**Supplementary Figure 6| Zonally-averaged rainfall responses to AGCM experiments.** Zonally averaged (10°W-30°E) precipitation from the experiment ‘MIROC\_20C’ (black line) and ‘MIROC\_21C\_extlatropics’ (red line). The bar graph represents the difference between the two experiments.

## Supplementary Table

**Supplementary Table 1 | A summary of SST sensitivity experiments.** The ECHAM6 model is forced by monthly climatological mean SSTs from GFDL-ESM2M, and a total of 20 ensemble runs with different initial conditions are carried out. The same experiments are also conducted using MIROC-ESM SSTs.

Name of experiment	Prescribed SST (from GFDL-ESM2M)
GFDL_20C	climatology (1970-1999), global
GFDL_21C	climatology (2070-2099), global
GFDL_21C_tropics	climatology (2070-2999) in tropics (30°S~30°N) + climatology (1970-1999) in extratropics (poleward of 30°N and 30°S)
GFDL_21C_extratropics	climatology (1970-1999) in tropics (30°S~30°N) + climatology (2070-2099) in extratropics (poleward of 30°N and 30°S)

The experiment names used in the main article can be understood as follows.

- Exp\_GFDL = “GFDL\_21C” – “GFDL\_20C” (Impact of global warming)
- Exp\_GFDL\_tropics = “GFDL\_21C\_tropics” – “GFDL\_20C” (Impact of tropical warming)
- Exp\_GFDL\_extratropics = “GFDL\_21C\_extratropics” – “GFDL\_20C” (Impact of extratropical warming)



## **Supplementary Note 1: Testing the performance of the NH differential warming index using observational data**

A similar statistical analysis to the one shown in the main manuscript is carried out with observational data to determine whether the NH differential warming index defined in this study can explain historical Sahel rainfall variations. The observed precipitation and sea surface temperature (SST) data used in this analysis were obtained from the Global Precipitation Climatology Center (GPCC)<sup>1</sup> and the extended reconstructed SST version 3 (ERSST v3)<sup>2</sup> datasets, respectively. The multi-linear regression analysis shows that our NH differential warming index can reproduce the observed Sahel rainfall variations with a high accuracy, performing even slightly better than other previously used SST indices, such as tropical SST indices (tropical Atlantic and Indo-Pacific), the relative subtropical Atlantic warming index, and the global interhemispheric gradient index (Supplementary Fig. 4). Given the successful reproduction of future Sahel rainfall trend using the NH differential warming index as shown in Supplementary Fig. 3a, this observational analysis emphasises that one simple hemisphere-wide SST index can serve as a unifying indicator of present and future Sahel rainfall behaviour.

## Supplementary Note 2: AGCM experiments

The performance of different versions of ECHAM in reproducing Sahel rainfall has been addressed in several previous studies. For example, ECHAM5 reproduces the observed summer (July-August-September) mean pattern and seasonal cycle of Sahel rainfall reasonably well<sup>3</sup>. The historical low-frequency variability of Sahel rainfall can also be accurately reconstructed by prescribing historical SSTs to the model<sup>4</sup>. The latest version of ECHAM (ECHAM6), which is used in this study, also shows a skillful prediction of Sahel rainfall in the decadal hindcasts<sup>5</sup>. This finding suggests that ECHAM6 is a reliable tool for a quantitative analysis of the Sahel rainfall.

It is also informative to examine the direct radiative impact of CO<sub>2</sub> increase (not the impact by changing the SST) on Sahel rainfall. Our SST-sensitivity experiment does not consider the direct enhanced radiative forcing by CO<sub>2</sub> increase on the continent, and therefore our result might underestimate the impact of CO<sub>2</sub> change on this monsoonal region. In fact, radiative heating by greenhouse gases is generally more prominent over the continent than the nearby oceans during summer due to the smaller heat capacity of the land surface; thus, the West African heat low and corresponding monsoonal flow is intensified, thereby increasing Sahel rainfall<sup>6</sup>. Additional AGCM experiments with increased CO<sub>2</sub> concentration (368 ppm → 538 ppm), but prescribed by fixed climatological 20<sup>th</sup> century SSTs from both GFDL-ESM2M and MIROC-ESM, are conducted to quantify the direct radiative CO<sub>2</sub> impact on Sahel rainfall. The results show that Sahel rainfall is enhanced independently of the GFDL or MIROC SSTs (Supplementary Fig. 5), which implies that the direct radiative forcing by CO<sub>2</sub> increase cannot explain the disparate future Sahel rainfall projections. Although the rainfall responses shown in Supplementary Fig. 5 might be slightly overestimated due to the fixed SST boundary condition (i.e., a stronger thermal contrast between ocean and land), the

magnitude of the rainfall increase is relatively weak compared to the impact of SST changes, particularly, that of extratropical SST changes (Figs. 3e and 3f in the main article). Therefore, the direct radiative CO<sub>2</sub> impact cannot be a dominant factor influencing future Sahel rainfall or a source of the model variability in projections of future rainfall.

## Supplementary References

- 1 Schneider, U. *et al.* GPCP's new land surface precipitation climatology based on quality-controlled in situ data and its role in quantifying the global water cycle. *Theoretical and Applied Climatology* **115**, 15-40 (2014).
- 2 Smith, T. M., Reynolds, R. W., Peterson, T. C. & Lawrimore, J. Improvements to NOAA's historical merged land-ocean surface temperature analysis (1880-2006). *J. Clim.* **21**, 2283-2296 (2008).
- 3 Bader, J. & Latif, M. The 1983 drought in the West Sahel: a case study. *Clim. Dyn.* **36**, 463-472 (2011).
- 4 Mohino, E., Janicot, S. & Bader, J. Sahel rainfall and decadal to multi-decadal sea surface temperature variability. *Clim. Dyn.* **37**, 419-440 (2011).
- 5 Gaetani, M. & Mohino, E. Decadal Prediction of the Sahelian Precipitation in CMIP5 Simulations. *J. Clim.* **26**, 7708–7719 (2013).
- 6 Haarsma, R. J., Selten, F. M., Weber, S. L. & Kliphuis, M. Sahel rainfall variability and response to greenhouse warming. *Geophys. Res. Lett.* **32** (2005).